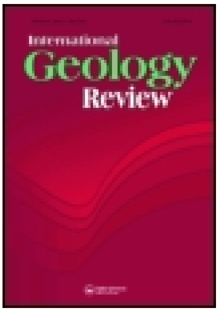

International Geology Review
Publication details, including instructions for authors and subscription information:
http://www.tandfonline.com/loi/tigr20

Cenozoic Left-Slip Motion along the Central Altyn Tagh Fault as Inferred from the Sedimentary Record

Zhengle Chen [a] , Xiaofeng Wang [a] , An yin [b] , Bailin Chen [a] & Xuanhua Chen [a]

[a] Institute of Geomechanics, Chinese Academy of Geological Sciences

[b] University of California, Los Angeles

Version of record first published: 14 Jul 2010.

To cite this article: Zhengle Chen, Xiaofeng Wang, An yin, Bailin Chen & Xuanhua Chen (2004): Cenozoic Left-Slip Motion along the Central Altyn Tagh Fault as Inferred from the Sedimentary Record, International Geology Review, 46:9, 839-856

To link to this article: http://dx.doi.org/10.2747/0020-6814.46.9.839

International Geology Review, Vol. 46, 2004, p. 839–856.

Cenozoic Left-Slip Motion along the Central Altyn Tagh Fault as Inferred from the Sedimentary Record

ZHENGLE CHEN,[1] XIAOFENG WANG,

Institute of Geomechanics, Chinese Academy of Geological Sciences, Beijing 100081, China

AN YIN,

Department of Earth and Space Sciences and Institute of Geophysics and Planetary Physics, University of California, Los Angeles, California 90095

BAILIN CHEN, AND XUANHUA CHEN

Institute of Geomechanics, Chinese Academy of Geological Sciences, Beijing 100081, China

Abstract

Several Cenozoic sedimentary basins are present along the central segment of the Cenozoic Altyn Tagh fault (ATF) that marks the northern boundary of the Tibetan Plateau. Field investigations reveal that basin sedimentation and subsequent deformation are controlled by left-slip motion along the Cenozoic ATF. In order to better understand the temporal and spatial interactions between the Altyn Tagh fault and the development of adjacent basins, we divided Cenozoic sedimentary sequences into three subunits based on lithologic variation and the presence of unconformities. From our own observations and regional correlations, we suggest that slip along the central ATF began in the Early Oligocene. Reconstruction of sedimentary relationships among the basin, slip along the fault, and offset topography suggests that the ATF experienced four stages of Cenozoic left-slip motion. The offset of a Late Miocene sequence and its possible correlation across the Altyn Tagh fault suggests 80–100 km left slip. This yields an average slip rate of 10–12.5 mm/yr assuming that the sequence was deposited at ~8 Ma.

Introduction

THE ENE-TRENDING Altyn Tagh fault (ATF) is a large intracontinental left-slip fault defining the northwestern edge of the Tibetan Plateau (Fig. 1). Its development has been considered to be an important mechanism for accommodating the growth and uplift of the Tibetan Plateau during the Indo-Asia collision (Molnar and Tapponnier, 1975; Burchfiel et al., 1989; Yin and Nie, 1996). The magnitude and rate of left-slip motion on the fault represents a key to assessing the relative importance between extrusion and distributed shortening during the Indo-Asian collision (Meyer et al., 1996, 1998; Ge et al., 1998; Shen et al., 2001; Cowgill et al., 2003; Gehrels et al., 2003a, 2003b). Although the Altyn Tagh fault system has been investigated by using satellite images (Tapponnier and Molnar, 1977; Peltzer et al., 1989; Meyer et al., 1996, 1998) and field investigations (Molnar et al., 1987; SSB, 1992; Rumelhart et al., 1999; Yue and Liou, 1999; Xu et al., 1999; Cowgill et al., 2000, 2003; Washburn et al., 2001; Yin et al., 2002), its detailed slip history and the distribution of left-slip motion along the fault remain controversial (Yin and Harrison, 2000; Yin et al., 2002; Yue and Liu, 1999; Yue et al., 2001; Ritts et al., 2003). A few estimations of the total displacement have been proposed from different sets of geologic piercing points, which range from about 120 km to more than 1000 km (Peltzer et al., 1989; SSB, 1992; Meyer et al., 1996; Wang, 1997; Guo and Xiang, 1998; Xu et al., 1999; Ritts and Biffi, 2000; Xiang et al., 2000; Meng et al., 2001; Yang et al., 2001; Yin et al., 2002; Cowgill et al., 2003; Gehrels et al., 2003a, 2003b).

Several Cenozoic sedimentary basins have developed between 90ºE and 92ºE along the central segment of the Altyn Tagh fault, from Manya south of the Altyn Tagh fault to Lapeiquan north of the fault (Fig. 2). These include, from northeast to southwest, the North Xorkol Basin, the Xorkol Valley fault-basin, the south Xorkol area, the Gebiling area, the Xorkol Basin, the Yitunbulake Basin, and the Kumutashi Basin (Fig. 2). Although some

[1]Corresponding author; email: chenzhengle@263.net

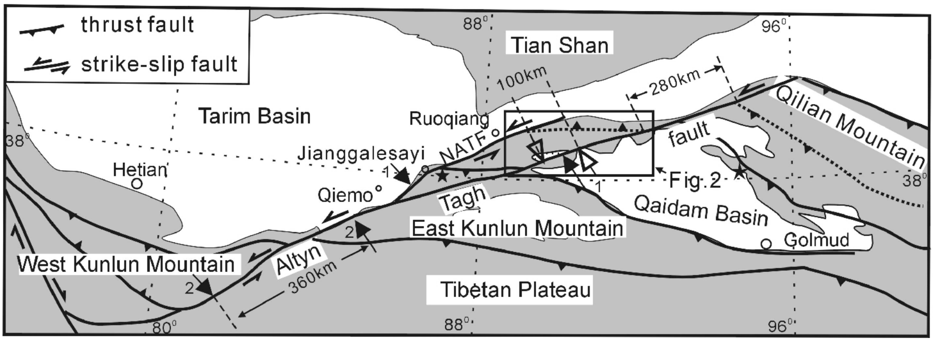

FIG. 1. Regional map of northwestern China showing the current location of the Altyn Tagh fault (ATF) in the northwestern edge of the Tibetan Plateau, and the relationship between the ATF and neighboring Tarim and Qaidam basins. This map is mainly modified from Yin et al. (2002) and Ritts and Biffi (2000). Several estimated results of the displacement along the ATF are shown in this map. The dashed line depicts a pair of oppositely dipping Cenozoic thrust systems on both sides of the ATF, suggesting 280 km offset along the eastern segment of the ATF (Yin et al., 1999). Five solid stars show the location of eclogites in the Altyn Tagh and northern edge of the Qaidam Basin, indicating 400 km offset along the ATF (Zhang et al., 2001). Solid triangular arrows represent piercing points of (1) Jurassic shoreline and (2) Jurassic shoreline aligning felsic plutons across the ATF, as proposed by Ritts and Biffi (2000), showing post-Jurassic 360 km left-lateral separation on the ATF. Open triangular arrows show dislocation of the outlet of the Xorkol Basin, indicating 80–100 km slip along the fault suggested in this paper. Abbreviations: NATF = northern Altyn Tagh fault.

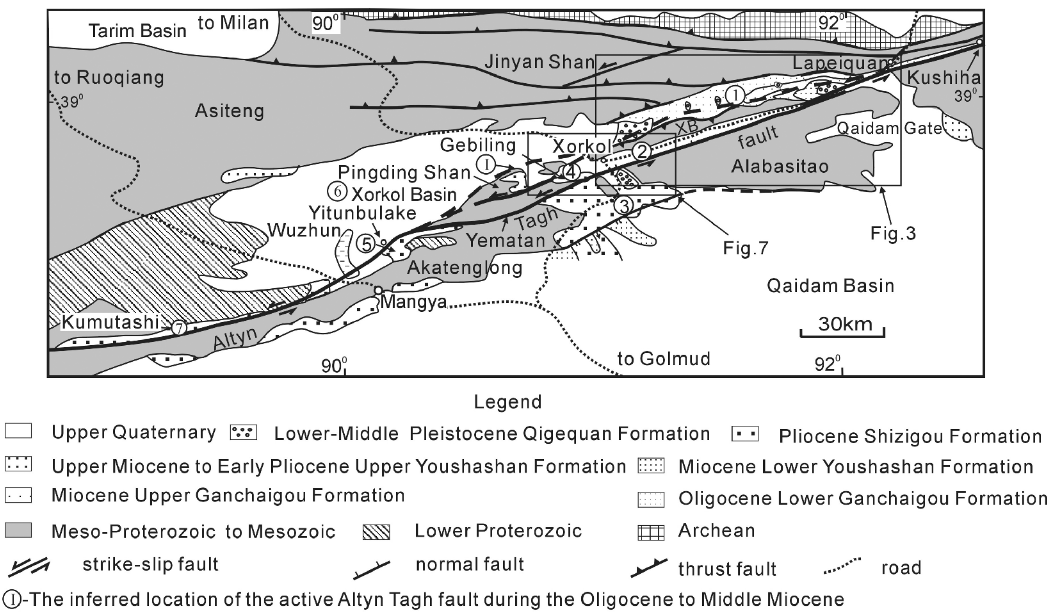

FIG. 2. Distribution of Cenozoic sedimentary basins along the central Altyn Tagh fault, modified from the regional geologic map completed by Xinjiang (1993) and Qinghai BGMR (1991), together with our field investigations. Abbreviations: XB = Xorkol Beishan. Legend: 1 = North Xorkol Basin; 2 = Xorkol Valley fault-basin; 3 = South Xorkol area; 4 = Gebiling area; 5 = Yitunbulake Basin; 6 = Xorkol Basin; 7 = Kumutashi Basin.

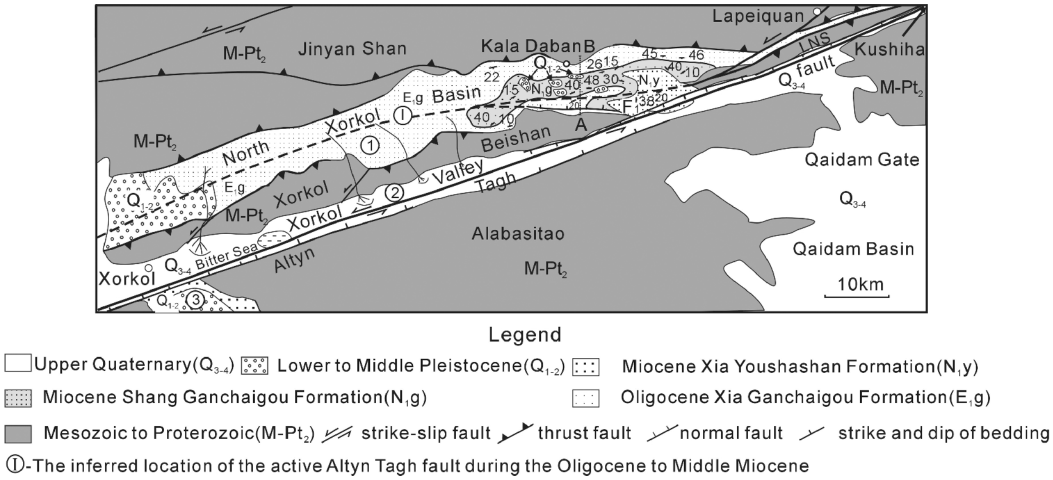

FIG. 3. Simplified geological map of the North Xorkol Basin and Xorkol Valley fault-basin. This map is modified from the regional geological map, 1:200,000 scale, of Xinjiang Province (Xinjing BGMR, 1981b), coupled with our field investigation in 1999 and 2001. The cross-section from A to B (Fig. 5) is shown in this map. Abbreviations: LNS = Lapeiquan Nanshan. Legend: 1 = North Xorkol Basin; 2 = Xorkol Valley fault-basin; 3 = South Xorkol area.

authors have focused on the Paleozoic to Mesozoic tectonic features along the Altyn Tagh fault (e.g., Xu et al., 1999), the Cenozoic basins have been poorly mapped and studied (Guo and Zhang, 1998; Li et al., 2002b). The study presented below results from an integrated investigation of interactions between Cenozoic basin fill and deformation related to the ATF strike-slip motion.

Lithostratigraphy and Structures of Cenozoic Basins

North Xorkol Basin

The North Xorkol Basin is bounded by the EW-trending Jinyan Shan thrust in the north, by the ENE-trending Xorkol thrust along the northern edge of the Xorkol Beishan, and by the Lapeiquan Nanshan in the south (Chen et al., 2003) (Fig. 3). This basin is ~150 km long and 8~10 km wide. Four lithostratigraphic units are recognized, based on an early geological map of the Xorkol Sheet (Xinjiang BGMR, 1981b) and our own field mapping in the summer of 2001. Unit 1, the Xia (Xia = lower in Chinese) Ganchaigou Formation, is composed of gypsum-bearing red conglomerates and sandy conglomerates interbedded with gray and yellow sandstones and mudstones. This unit is of Oligocene age based on the presence of freshwater ostracods (Xinjiang BGMR, 1993). Alluvial and fluvial fan facies were deposited along the northern and southern basin boundaries, whereas lacustrine facies were deposited in the center of the basin. Unit 2, the Miocene Shang (Shang = upper in Chinese) Ganchaigou Formation, consists of grey to yellow and brown mudstones and siltstones locally interbedded with coal-bearing mudstones; these strata are of lacustrine origin. Unit 3, the Miocene Xia Youshashan Formation, consists mainly of yellow conglomerates with brown and red mudstones, siltstones, and sandstones, which in general are not well sorted with angular pebbles and boulders, suggesting alluvial- and pluvial-fan settings. Unit 4, the Lower Quaternary Qigequan Formation, was newly recognized in this basin during our field study through regional comparison of both composition and texture with sediments in the western Qiadam Basin south of the Altyn Tagh fault (Qinghai BGMR, 1991), as well as its unconformable contact with lower sections. It is mainly composed of light grey, sandy conglomerates interbedded with grey and yellow sandstones and siltstones. The sediments are poorly sorted and pebbles poorly rounded. Pebbles in the conglomerates are mostly limestone, similar to rocks exposed in the hanging walls of the Jinyan and Xorkoli thrusts around the basin. Flat-lying Quaternary conglomerates lie directly over folded Tertiary

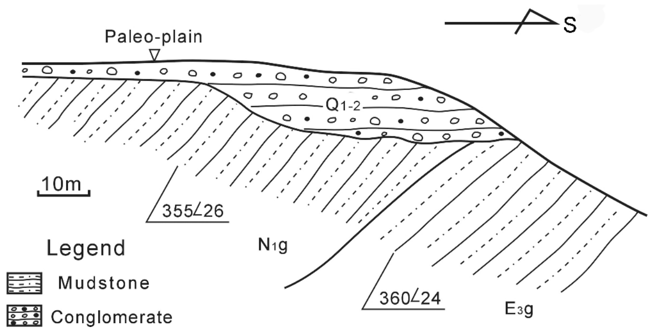

FIG. 4. Unconformity contact between the Lower Quaternary conglomerate and the Tertiary mudstone. Legend: E_3g = Oligocene Xia Gangchaigou Formation; N_1g = Miocene Shang Gangchaigou Formation; $Q_{1\text{-}2}$ = Lower–Middle Pleistocene Qigequan Formation.

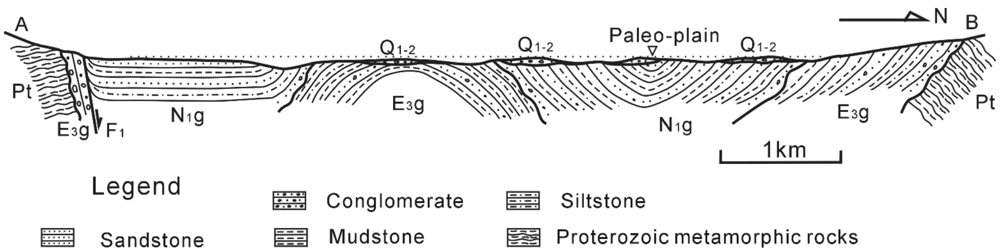

FIG. 5. Cross-section in the Kala Daban area, North Xorkol Basin, showing the oven-shaped syncline of Tertiary units capped by gently dipping Lower Quaternary conglomerates. Tertiary sediments mostly unconformably overlie Proterozoic metamorphic rocks on both sides of the basin. The location of this cross-section is shown in A–B, Figure 3. Legend: E_3g = Oligocene Xiar Gangchaigou Formation; N_1g = Miocene Shang Gangchaigou Formation; $Q_{1\text{-}2}$ = Lower–Middle Quaternary; Pt = Proterozoic.

units (Fig. 4), making a distinguishable topography because of the resistant nature of the calcite-cemented conglomerates in the younger unit.

The Tertiary strata are gently folded. The fold axis trends ENE parallel to the long dimension of the basin and the basin-bounding thrusts. The dip angle of the bedding is typically less than 30°, but locally becomes steeper toward its margins against the thrusts. An oven-shaped syncline can be observed (Fig. 5). The fold series are overlain in angular unconformity by the Lower Pleistocene Qigequan conglomerates (Figs. 4 and 5). This unit also overlies the Jinyan and Xorkoli thrusts, attesting that the thrusts are no longer active.

A north-dipping normal fault was newly discovered close to the southern edge of the basin during our field observation (F_1 in Figs. 3 and 5). The footwall is composed of the Oligocene Xia Ganchaigou Formation; the hanging wall is made of the Miocene Shang Ganchaigou Formation. The dip of the bedding in the hanging wall increases toward the fault (Fig. 5), suggesting syn-sedimentary faulting. Small syn-sedimentary normal faults are also found in the Miocene Shang Ganchaigou Formation and the Xia Youshashan Formation, indicating a transtensional tectonic environment during the Miocene.

The narrow, elongate geometry of the North Xorkol Basin and the distribution of Cenozoic sediments indicate that the formation and filling process of the basin was controlled by a major strike-slip fault. As described later, a large-scale strike-slip fault, possibly the main trace of the active ATF in the Oligocene, may lie below the basin or along its southeastern edge. This speculated tectonic configuration of the ATF—in and prior to—the Oligocene relationship may be similar to the present transtensional relationship between the active ATF and the modern Xorkol Valley fault basin (Fig. 2).

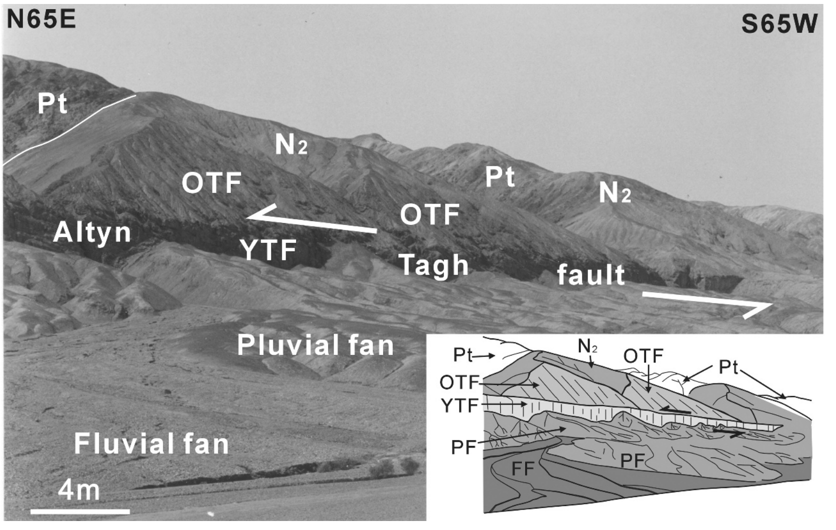

FIG. 6. Two phases of triangular facets developed along the active Altyn Tagh fault in the southeastern edge of the Xorkol Valley fault-basin. The older triangular facet is cut by a new developed triangular facet. Pluvial and fluvial fans are cut by the younger facet. Abbreviations: OTF = older triangular facet; YTF = younger triangular facet; N_2 = Pliocene Zhizigou Formation; Pt = Proterozoic; PF = Pluvial fan deposit; FF = Fluvial fan sediment.

Xorkol Valley Basin

The ENE-trending Xorkol Valley, a narrow fault-bounded depression, is 100 km long and 1–5 km wide. It is bounded by the active Altyn Tagh fault along the northern margin of the Alabasitao massif in the south, and the south slope of the Xorkol Beishan in the north (Figs. 2 and 3). Three sedimentary sequences filling the fault valley were distinguished during our field investigation. The youngest unit consists of active, poorly consolidated Holocene alluvial fans, mostly developed on both sides of the valley. The middle unit is exposed by erosion along the central valley, and is composed of a series of red-to-dark purple mudstones deposited in a lacustrine environment. They are flat-lying in the center of the valley but become gently tilted near the ATF. This redbed sequence is capped on top by a gravel layer. TL dating of the gravel layer yields ages of 22 ka, 79 ka, and 100 ka (SSB, 1992; Li et al., 2002a). These ages suggest that the gravel unit was deposited in the late Pleistocene. The oldest sedimentary sequence in the Xorkol Valley consists of gypsum-bearing red mudstones and sandy mudstones, which are sparsely exposed along the active trace of the ATF. The age of the unit is not known, although it has been assigned to a Middle to Late Tertiary age based on regional lithologic correlation (Xinjiang BGMR, 1981b). In order to determine the age of this unit, we dated one gypsum sample from this unit (sample 6151-3) using the electron spin resonance method, which gave an age of 1.71 Ma (Chen, 2002). This suggests that the redbed unit in the Xorkol Valley is Pleistocene in age.

The main trace of the active ATF lies along the center of the valley. It curves southeastward to bound the basin and forms a series of NW-facing triangular facets with a normal-slip component. At least two phases of triangular facets can be recognized along the fault (Fig. 6). The older ones are tall, uplifted, and dissected by streams, whereas the younger ones are short and relatively continuous laterally. The young facets cut the older ones. The Altyn Tagh fault continues southwestward into the South Gebiling Valley where the active ATF cuts several alluvial fans (SSB, 1992; Washburn et al., 2001).

Li et al (2002a) has proposed that the long, narrow Xorkol Valley results from transpression started in the Pliocene, and modern basin morphology was created during the Late Pleistocene. The valley is also suggested to be controlled by thrust faults on both sides (SSB, 1992). However, our field observations and regional data do not support these suggestions. Neotectonic features as described above along the Altyn Tagh fault are more compatible with

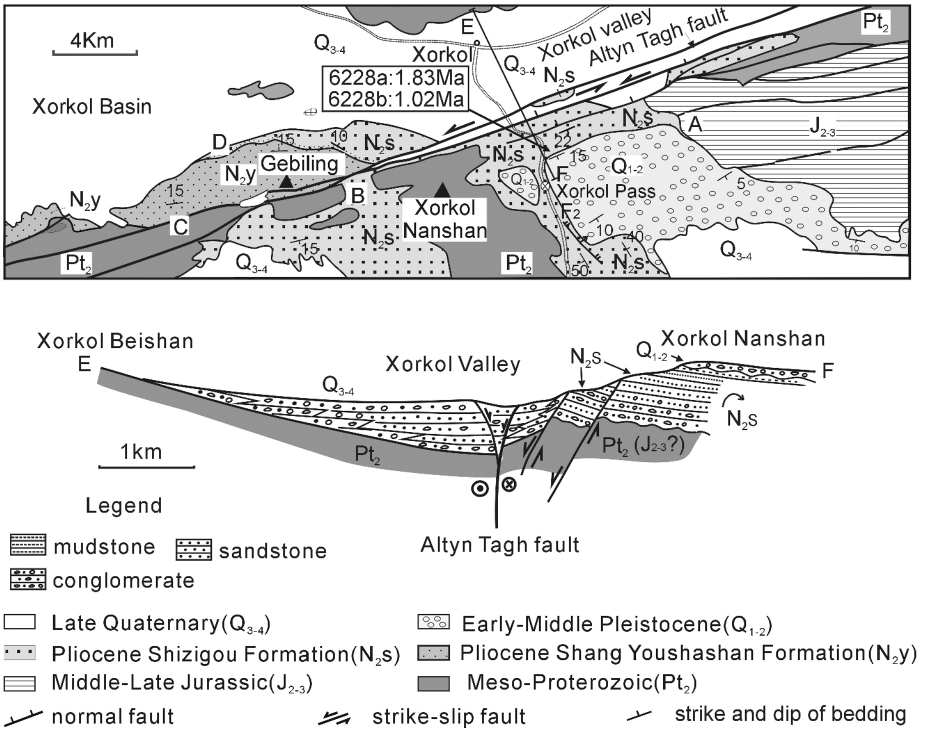

FIG. 7. Simplified geological map in the Xorkol area. Section locations of Figures 8 and 10 are shown by A, B and C, D on this map. Profile E–F shows structure of Quaternary deposits in the Xorkol Valley fault-basin and Tertiary sediments in the south Xorkol area, and the more than 400 meter difference in topography between the Xorkol Valley with the Xorkol Nanshan. Tilt-uplifting and normal-faulting resulted in the formation of more than 400 meters difference in elevation between the Xorkol Valley and the Xorkol Nanshan. Sample 6228a yields 1.83 Ma and sample 6228b yields 1.02 Ma ESR (Electron Spin Resonance) ages of gypsum collected in WNW-trending fissures.

transtension along the fault. This interpretation would explain the southeastward tilting of the Alabasitao massif in the Xorkol Nanshan south of the Altyn Tagh fault. Tilting is expressed by denudation of Pliocene–Middle Pleistocene strata. We also speculate that the South Gebiling valley and Yematan valley result from transtensional tectonics along the left-slip Altyn Tagh fault. We suggest that the Xorkol valley basin began to form during the Late Pleistocene because: (1) the youngest strata cut by the ATF in the basin are Early to Middle Pleistocene in age; and (2) sedimentary facies and paleo-current indictors show that paleo-drainage systems were flowing across the main trace of the ATF from the Pliocene to Early and Middle Pleistocene. The relatively small topographic relief (~400 m) also implies youthfulness of the Xorkol Valley (see profile E–F in Fig. 7).

South Xorkol area

The Cenozoic sedimentary units south of the Altyn Tagh fault in the Xorkol Pass area are truncated by the active ATF (Figs. 7 and 8). Two Cenozoic lithostratigraphic units were mapped by Xinjiang BGMR (1981b) in the South Xorkol area (Figs. 7 and 8): the older > 1000 m thick Pliocene Shizigou Formation, and the younger 80 m thick Lower to Middle Pleistocene Qigequan Formation in the map of the Xorkol sheet (Xinjiang BGMR, 1981b). The ages of the two units were determined by magnetostratigraphic analysis (CNPC, 1992; Liu et al., 1997; Wan et al., 1999). An angular unconformity between these two units was found in our field investigation and was also reported by Xinjiang BGMR (1981b).

The Shizigou Formation can be divided into three lithostraigraphic packages. Unit 1 consists

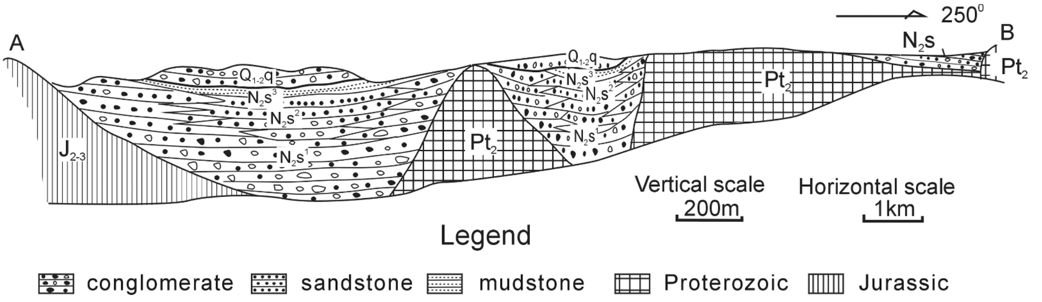

FIG. 8. Profile across the South Xorkol Area, showing characteristics of a typical channel filling series. The vertical scale is 6× the horizontal scale in order to show the texture inside the basin more clearly. See Figure 7 and the map legend for explanation. Legend: $Q_{1\text{-}2}$ = Lower–Middle Pleistocene Qigequan Formation; N_2s = Pliocene Shizigou Formation; $J_{2\text{-}3}$ = Middle–Upper Jurassic; Pt_2 = Proterozoic.

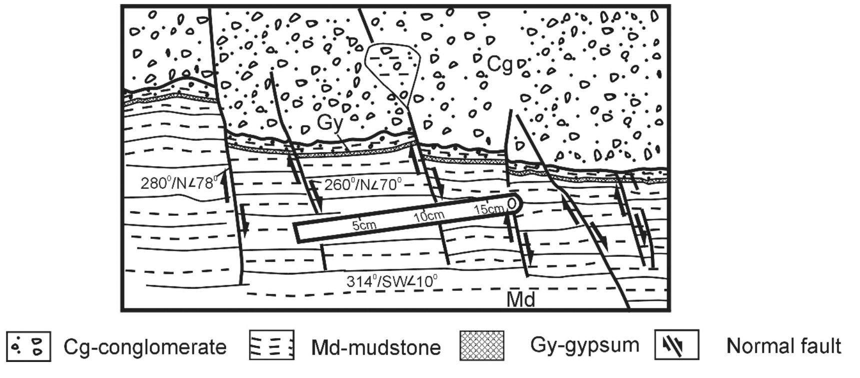

FIG. 9. Normal faults parallel to the main trace of the active Altyn Tagh fault in the Pliocene Shizigou Formation are well developed. This caption is modified from a field photo, and the ruler in the picture is shown for scale.

primarily of greyish white to yellow cobble-sized conglomerates with lenticular gravel-bearing sandstones. Pebbles are mainly gneiss, limestone, and schist that are particularly prevalent in the basal part of the unit (>70%). The percentage of the pebble clasts decreases systematically upsection from nearly 95% to 45% from the base to the top. This is associated with an increase in the roundness of the pebbles. Unit 2 is mainly composed of 40–60% conglomerates interbedded with pebble sandstones and pebble-bearing mudstones. Unit 3 contains dominantly greyish white to greyish green and yellow mudstones interbedded with less than 30% conglomerates. Pebbles in the conglomerates contain >50% quartzite. The upward fining of the Shizigou Formation indicates a systematic change in sedimentary environment, from the alluvial fans at the bottom to fluvial channels at the top. Most of the paleocurrent indicators such as cross-bedding and pebble imbrication show a northwest-derived source for the Shizigou Formation in the South Xorkoli area. Well-developed synsedimentary growth faults and normal faults (Fig. 9) parallel the main trace of the ATF, indicating a transtensional tectonic setting during deposition of the unit. Striations mark some fault planes, showing left-lateral normal faulting.

The Qigequan Formation consists mainly (> 85%) of grey conglomerates, locally interbedded with lenticular sandstone beds. Pebbles in the conglomerates typically contain well-rounded pebbles. A relatively flat erosional surface is well preserved at the top of the Qigequan Formation.

Subvertical WNW-striking (290°) extensional cleavages are widespread near Xorkol Pass in the Shizigou Formation (Fig. 7). Gypsum veins are developed perpendicularly to the cleavage, suggest-

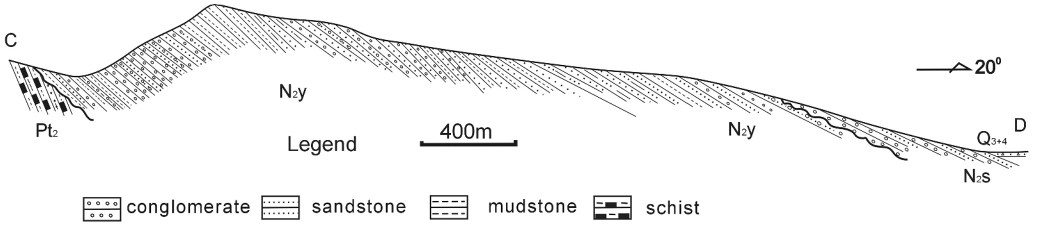

FIG. 10. Cross-section showing Upper Cenozoic sediments in the Gebiling area (modified from the 1:200,000 regional map of the Xorkol sheet of Xinjiang Province, 1981b). Legend: Q_{3+4} = Upper Pleistocene to Holocene; N_2s = Pliocene Shizigou Formation; N_2y = Pliocene Shang Youshashan Formation; Pt_2 = Proterozoic.

ing that their development may be coeval. Two gypsum samples were collected from the cleavages for electron-spin-resonance dating. They yield ages of 1.02 Ma (sample 6228b) and 1.82 Ma (sample 6228a), respectively (Chen et al., 2002a, 2002c). These ages indicate that the cleavage formed in the Early Quaternary. The presence of a WNW-trending normal fault (F_2 in Fig. 7), WNW-trending cleavage, and a drag fold in the Pliocene mudstone all suggest compression in a WNW-ESE direction.

Gebiling area

Upper Cenozoic sediment in the Gebiling area can also be divided into two units: the Pliocene Shang Youshashan Formation and the Pliocene Shizigou Formation with a thickness of over 1200 meters, with the bottom not exposed (Figs. 6 and 10; Xinjiang BGMR, 1981a). The Shang Youshashan Formation might be Upper Miocene sediment according to paleomagnetic data in the west Qaidam Basin (CNPC, 1992; Liu et al., 1997; Wan et al., 1999). The lower part of the Shang Youshashan Formation is characterized by brown to yellow conglomerates interbedded with yellow sandstones and mudstones. Red siltstones and mudstones as the major component in the upper part are locally interbedded with lenticular yellow conglomerates. Gypsum grew on the surface of the bamboo-bearing mudstone on the topmost, indicating a relatively dry-season lacustrine environment. This change from conglomerate to sandstone to mudstone upward shows a complete sedimentary cycle of a fault-bounding lake series from alluvium or talus at the bottom to lacustrine on the top. The Shizigou Formation here is mostly composed of yellow to grey conglomerates with sandstones, overlying the Shang Youshashan Formation with angular unconformity (Fig. 10).

Xorkol Basin

The Xorkol Basin is expressed in topography as a large depression inside the Altyn Tagh Range. It is mostly filled by Upper Quaternary alluvial fan deposits. Huge, prominent alluvial bajadas are developed along the southern and northern margins of the basin. Wuzhun Lake is the southernmost part of the basin and is cut by the active ATF (Fig. 2). The origin of the Xorkol Basin is poorly understood. Guo and Zhang (1998) proposed a pull-apart-basin model for its formation. However, neither satellite-image interpretations nor our field observations support this model. Based on the morphology of the basin, we argue that Xorkol Basin originated from incision of a river system during the Late Tertiary. The outlet of this basin is located in Wuzhun Lake, which has been offset left-laterally by the ATF. Eroded sediments of the valley should have been shed into the Qaidam Basin. As illustrated below, the erosional valley evolved into a depositional basin during the Middle to Late Quaternary as a consequence of closure of its outlet by left-lateral juxtaposition of the Akatenglong massif along the Altyn Tagh fault (Fig. 2).

Yitunbulake and Kumutashi basins

The Late Cenozoic Yintunbulake basin lies along the northern edge of the Akatenglong Shan against the Altyn Tagh fault (Fig. 1). The northwestern part of the basin is truncated by the active ATF. Qinghai BGMR (1986a) recognized three sedimentary units in the basin. The lower unit, the Xia Youshashan Formation, is composed of red mudstones and siltstones interbedded with sandy mudstones and local conglomerates. They lie unconformably over Proterozoic gneisses and Early Paleozoic granites. The younger Shang Youshashan Formation contains a large portion of conglomerates, whereas the over-

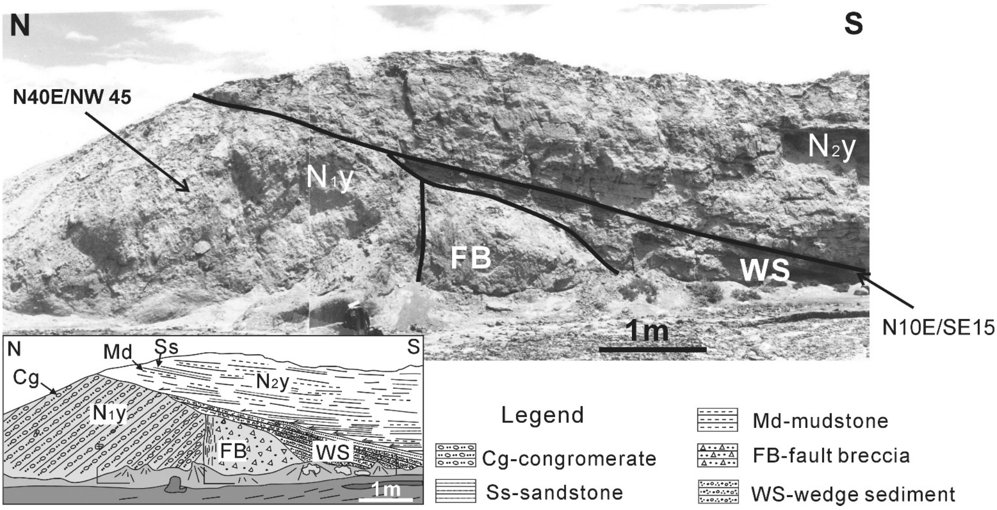

FIG. 11. Unconformity between the Miocene Xia Youshashan Formation and the Pliocene Shang Youshashan Formation in the Yitunbulake Basin. The backpack in the picture is about 20 cm in width. Legend: N_2y = Pliocene Shang Youshashan Formation; N_1y = Miocene Xia Youshashan Formation; Pt_2 = Proterozoic.

lying Shizigou Formation is composed mainly of gray mudstones interbedded with conglomerates and sandstones. Contacts of these three units are unconformable (Fig. 11).

The Kumutashi Basin is 60 km long and < 2 km wide. It is also cut by the ATF at its southeastern end (Fig. 1). Deposits in the basin consist of conglomerates and sandstone lenses, which can be correlated with the Shizigou Formation. They rest directly over Proterozoic gneisses (Xinjiang BGMR, 1993). The narrow, elongated geometry of the Yintunbulake and Kumutashi basins implies that both may have originated as releasing bends along the ATF.

Synthesis of Cenozoic Sedimentary Sequences

A general lithostratigraphic correlation of Cenozoic sedimentary sequences along the central segment of the Altyn Tagh fault can be established, based on the composition of sediments, sedimentary facies, and the internal unconformities (Fig. 12). The lowest unit is exposed in the North Xorkol Basin where sedimentary facies change gradually from alluvial and fluvial fan at the base, to lacustrine in the middle, and finally to alluvial and fluvial fan facies at the top. The middle unit is composed of the Upper Miocene to Lower Pliocene Shang Youshashan subunit, the Pliocene Shizigou subunit, and the Qigequan subunit. The lowermost subunit shows a facies change from alluvial fan at the bottom to lacustrine deposition in the top. The middle subunit displays a change from alluvium or talus deposits at the bottom to fluvial sedimentation in the top. The youngest Qigequan subunit is composed of mainly alluvial or pluvial sediments. The Upper Quaternary subunit in the uppermost section is mostly pluvial, alluvial fan, and lake deposits along the active trace of the ATF.

Estimates of Cenozoic Offsets along the ATF

Offset of a uniform strike-slip basin

As described above, the Cenozoic Yitunbulak Basin is exposed along the ATF and is cut at its northwestern end by the active ATF. There, basin sediments are directly juxtaposed against the Precambrian basement. Additionally, Upper Cenozoic sedimentary rocks in the Kumutashi Basin, although poorly constrained in age, extend along the northwestern side of the ATF and unconformably overlie Precambrian basement. The basin is cut by the Altyn Tagh fault at its southeastern end.

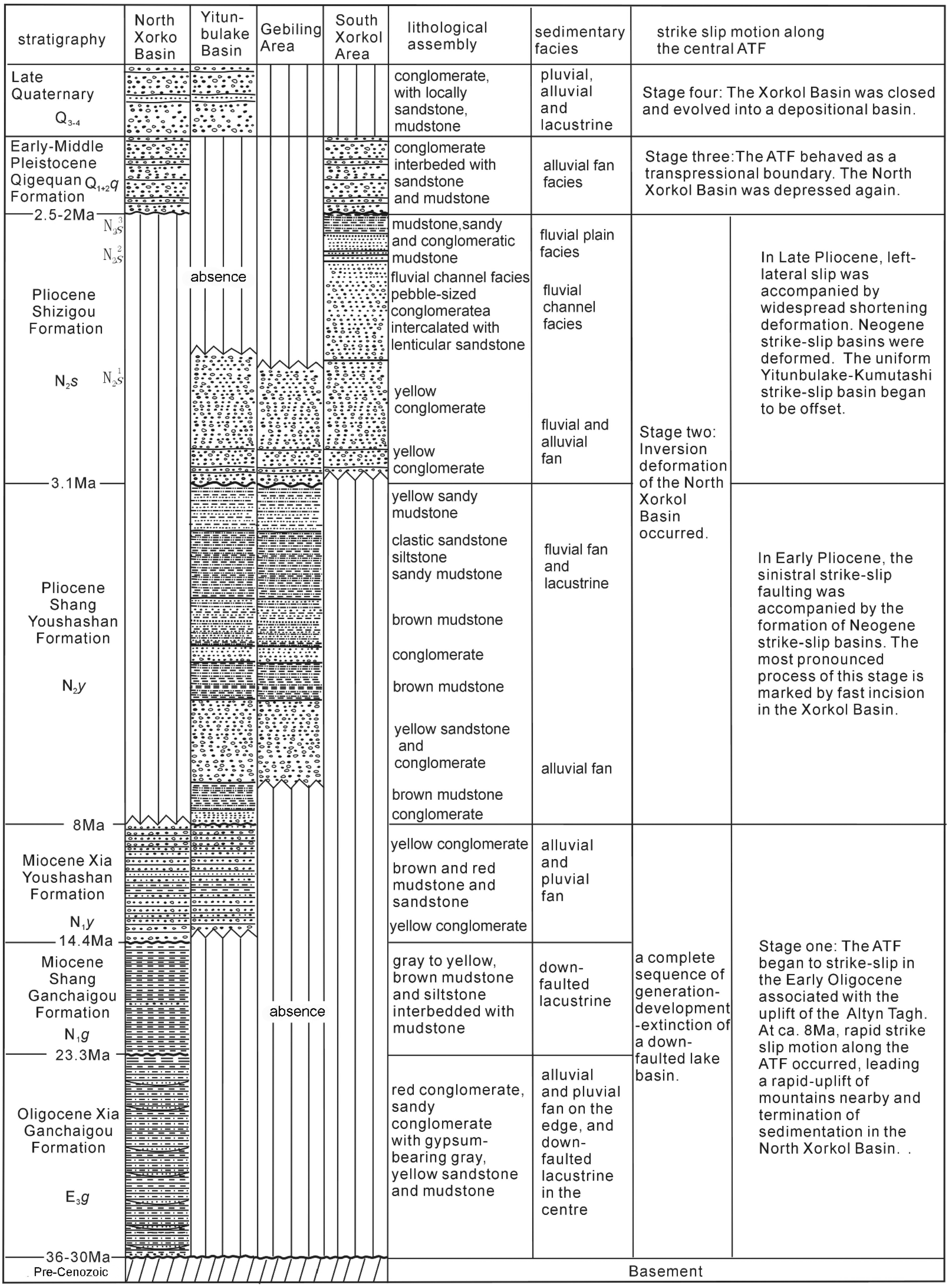

FIG. 12. Cenozoic sedimentary features and tectonic evolution along the central Altyn Tagh fault. The vertical scale of the stratigraphic column is based on the thickness of the strata measured during our field investigation and the geological map (1:200,000 scale) completed by Xinjiang (1981a, 1981b) and Qinghai BGMR (1986). The boundary ages between the Cenozoic units are cited from data in the Qaidam Basin by Huang et al. (1996).

Based on the above geologic relationships, we argue that the Neogene sediments exposed in the Yitunbulak and Kumutashi basins were deposited initially in a unified strike-slip basin formed during the Late Miocene and Early Pliocene along the Altyn Tagh fault. This basin was subsequently cut off and sliced by the ATF. This correlation requires that more than 80 km of left-slip has occurred along the central ATF since the Late Pliocene (Fig. 2; see also Fig. 14D).

Outlet of the Xorkol Basin and its correlation with channels in the South Xorkol area

We interpret Neogene sedimentary rocks exposed in the South Xorkol area south of the Altyn Tagh fault to have been deposited in fluvial meandering environments (Fig. 8). This interpretation has important implications for paleogeographic evolution of the Xorkol Basin during the Pliocene and Quaternary. Because no similar lithologic units exist between Neogene sedimentary rocks in the South Xorkol area south of the ATF and those in the Gebiling area north of the fault, we suggest that the drainage systems, as preserved in the South Xorkol area, may correspond to the outlet of a river valley that is occupied by the Xorkol Basin. As discussed earlier, the Xorkol Basin may have originated from an erosional valley during the Late Neogene. Outlet channels may have formed by incision of rivers into basement rocks, which allowed eroded materials to be transported southward across the Altyn Tagh fault into the western Qaidam Basin. Thus, the present position of the drainage system in the South Xorkol area may have resulted from a northeastward shift, with respect to rocks north of the Altyn Tagh fault, by continuous left-lateral strike-slip motion. This interpretation requires that the outlet channel system in the south Xorkoli area was originally located downstream of the Xorkol Basin. The composition of the pebbles in the Shizigou Formation in the South Xorkol area is similar to that of rocks exposed in the mountain ranges around the Xorkol Basin. This further supports the hypothesis that sediments in the south Xorkol area were derived from mountains around the Xorkol Basin north of the Altyn Tagh fault. Stream erosion had turned the Xorkol Basin into an intramountain depositional center during the Late Pliocene and Quaternary. The above reconstruction yields 80–100 km left-lateral offset along the central ATF during Pliocene–Quaternary time (Fig. 2; see also Fig. 14D).

A Four-Stage Model for the Slip History of the ATF

Our field investigations across the central Altyn Tagh, together with basin analyses, Electron Spin Resonance (ESR) dating of gypsum, and deformation and depositional history of Cenozoic sedimentary basins, allow us to reconstruct relationships among motion along the ATF, basin evolution, and development of paleotopography. In the following, we propose a four-stage strike-slip model for the evolution of the central ATF during the Cenozoic (Figs. 13 and 14).

Stage 1 (Oligocene to Middle Miocene, 36.5–8 Ma)

In the Early Oligocene, the ATF was transtensional, resulting in the formation of the North Xorkol Basin (similar to the present-day Xorkol Valley). This was accompanied by the uplift of the whole Altyn Tagh Range, although the magnitude of the uplift might have been small (Chen et al., 2001). The main trace of the Oligocene ATF may have bounded or was located inside the basin, causing its development as a narrow and elongate feature (Figs. 13A and 14A). Alluvial and pluvial fans developed along the edge of the basin that was bounded by the paleo-Altyn Tagh fault, which may have been associated with normal faults to accommodate transtension (i.e., fault F_1 in Figs. 3 and 5). Lakes probably formed in front of the major alluvial and fluvial fans distant from the mountain fronts, where fine-grained lacustrine sediments were deposited under relatively dry climatic conditions.

In the Early Miocene (the Shang Ganchaigou time period), sedimentation was limited to the center of the basin under relatively wet climatic conditions. As the ATF continued transtensional motion, the depositional center in the basin migrated toward the NNE. In the Middle–Late Miocene (Shang Youshashan time period), alluvial and fluvial fan deposits were limited to its northeastern part. Regional deformation and rapid strike-slip motion along the ATF occurred at ~8 Ma (Chen et al., 2002; Chen et al., 2002b), causing a rapid uplifting of mountains nearby and termination of sedimentation in the North Xorkol Basin.

Stage 2 (Late Miocene to the end of Pliocene, 8–2.5 Ma)

Tertiary folds in the North Xorkol Basin were developed in association with rapid incision of the

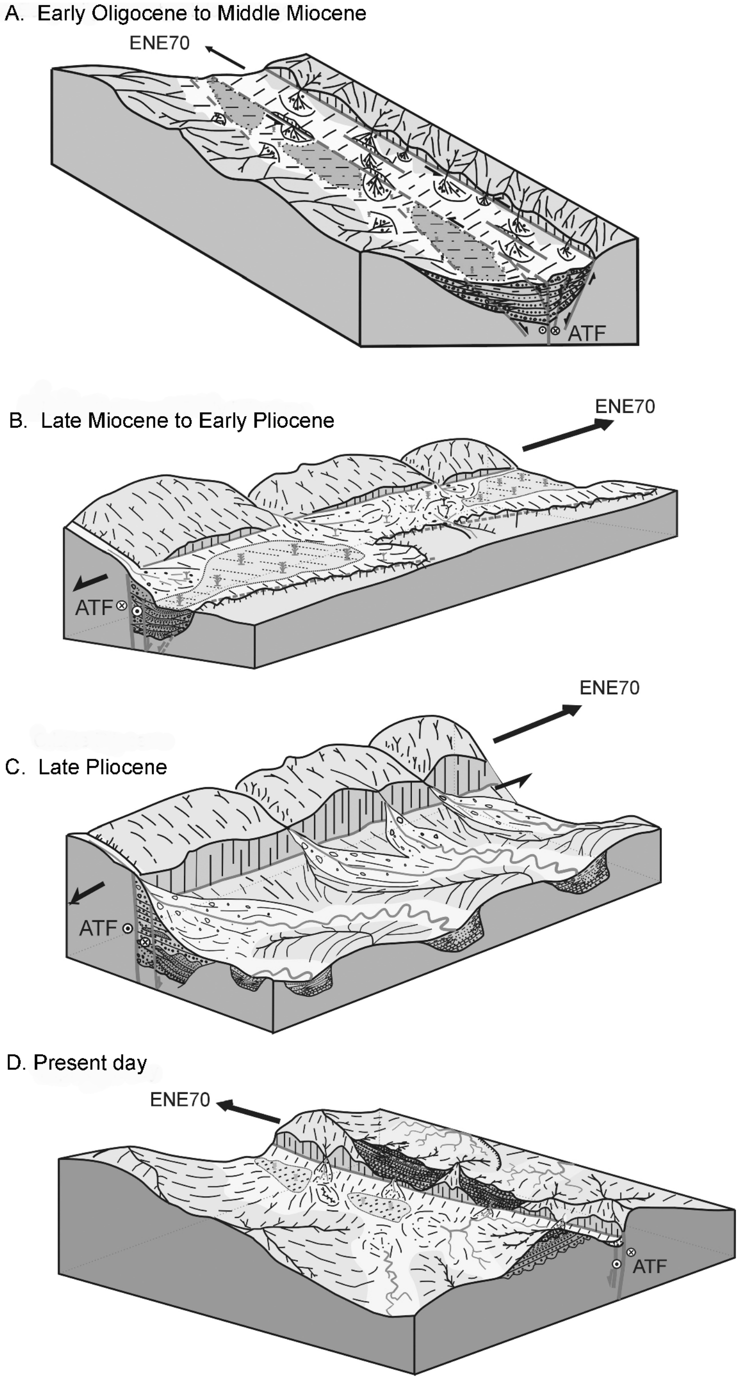

FIG. 13. Reconstruction showing the relationship among slip along the ATF, sedimentation in basins, and the paleotopography, indicating four-stage strike-slip motion along the central ATF. A. Early Oligocene to Middle Miocene. B. Late Miocene to Early Pliocene. C. Late Pliocene. D. Present. Abbreviations: ATF = Altyn Tagh fault. See text for explanation.

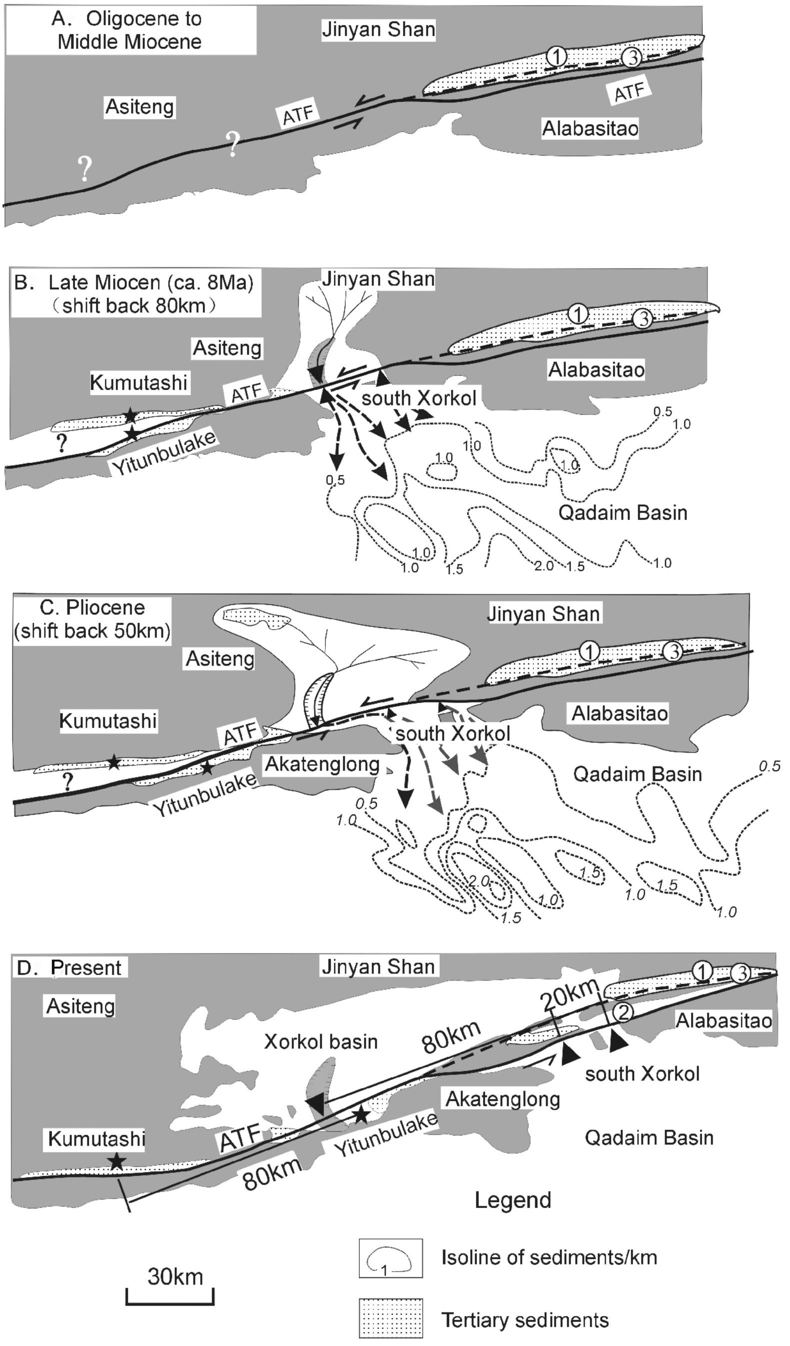

FIG. 14. Late Cenozoic strike-slip history along the central segment of the Altyn Tagh fault. The offset points of Tertiary sedimentary basins are marked by solid stars. The displacement of a proposed drainage outlet and its offset counterpart for the Xorkol Basin are marked by solid triangles. Isopach of the western Qaidam Basin is cited from Huang et al. (1996). A. Oligocene to Middle Miocene. B. Late Miocene (~8 Ma). C. Pliocene. D. Present. Abbreviations: ATF = Altyn Tagh fault. Legend: 1 = North Xorkol Basin; 2 = Xorkol Valley fault-basin; 3 = inferred location of the active Altyn Tagh fault during the Oligocene to Middle Miocene.

Xorkol Basin and sedimentation in the far-western Qaidam Basin. Meanwhile, strike-slip basins were created along releasing bends of the ATF (i.e., Gebiling, Yitunbulake, and Kumutashi basins) (Figs. 13B and 14B). In the Late Pliocene, Neogene strike-slip basins along the main fault trace were deformed by transpressional tectonics, causing folding and faulting of the Shang Youshashan Formation in the Gebiling, Yitunbulake, and Kumutashi areas and producing an unconformity between the Youshashan and Shizigou formations. The northwest side of the fault block was topographically higher than the southeast side along the central ATF. Several drainages cut across the Altyn Tagh fault, along which sediments were transported southwestward to the western Qaidam Basin. The Pliocene Shizigou Formation in the South Xorkol area was a result of river incision and basin fill, providing a geologic link between the Altyn Tagh Range and the Qaidam Basin (Figs. 13C and 14C).

In the beginning stage, the South Xorkol area was located at the upper reaches of the drainage system. Most of the sediments were derived from a nearby mountain front, resulting in deposition of ill-sorted, poorly rounded conglomerates. Subsequently, incision and offset of the source region by the Altyn Tagh fault stretched the length of the river course and the distance between the mountain front and the South Xorkol area. As a result, the basin in the South Xorkol area received sediments of more distal facies characterized by better sorted, more rounded, and relatively fine grained sedimentary deposits. As left-slip motion on the Altyn Tagh fault continued, the Yitunbulake-Kumutashi Basin was offset, and the outlet of the Xorkol Basin was cut and translated by the fault northeastward.

Stage 3 (Early to Middle Pleistocene)

At the end of the Neogene, most Cenozoic basins began to be uplifted. All river channels ceased to develop, and sedimentation was limited to a few loci such as the South Xorkol area, which was filled by alluvial fan deposits of the Lower–Middle Pleistocene Qigequan conglomerates, with provenance from a nearby mountain front. Reduced extent of sedimentary basins in the region, the presence of WNW-trending normal faults and cleavages in the South Xorkol area, and the development of thrusts along the Milan River along the northern edge of the Altyn Tagh range (Chen, 2002; Chen et al., 2002a) all imply a decrease in the normal component of transtension along the Altyn Tagh fault and regional NW-WNW–SE-ESE compression. The North Xorkol Basin subsided, resulting in the deposition of the Pleistocene Qigequan conglomerates resting gently on folded Tertiary sediments.

Stage 4 (Late Pleistocene to present)

Left-slip motion on the ATF has become localized and caused narrow valleys such as the Xorkol and Yematan to be developed. Left-lateral strike-slip of the ATF, accompanied by a minor normal component, shaped the modern topography along the central ATF. A change in the relative elevation between the Altyn Tagh range to the north and the Qaidam Basin to the south across the ATF occurred in the Xorkol Pass area (Fig. 8): the Altyn Tagh range immediately north of the fault lies > 400 m lower than the western edge of the Qaidam Basin (Figs. 13D and 14D). The Xorkol Basin was shut off as a consequence of left-lateral juxtaposition of the Akatenglong massif, causing it to evolve into an isolated depositional basin. The relatively uniform shape of the Late Cenozoic Yitunbulake-Kumatashi Basin was continuously torn off by the ATF, and the southeastern part of the basin was dislocated northeastward about 80–100 km to its present location.

Discussion

Change of location of the Altyn Tagh fault

As mentioned above, we argued that the formation of the North Xorkol basin was controlled by a large strike-slip fault, similar to the relationship between the present-day ATF and the Xorkol Valley basin (Fig. 1). The inferred paleo–Altyn Tagh fault may extend northward to the Lapeiquan area, turning into a thrust fault between the Ordovician Lapeiquan Group and the Xia Ganchaigou Formation. It joined the northeastern end of the active ATF in the Kushiha area, and is covered by the Qigequan conglomerates in the southwestern part of the basin. Toward the southwest, the inferred strike-slip fault might either join the present-day inactive normal fault developed along the northwestern edge of the Gebiling Shan and Pingding Shan, or connect with the active ATF in the Yematan area (Figs. 1 and 2). Lithostraigraphic evidence supports our idea of a concealed strike-slip fault beneath the North Xorkol Basin. Rocks exposed on the south side of the basin, the Xorkol Beishan, are dominantly Precambrian limestone, which are very different in lithological assemblages, textures, deformational styles, and metamorphic features from those exposed on the north side of the basin in the Jinyan Shan. There the rocks are mainly Ordovician schists and volcanic rocks (Xinjiang BGMR, 1981b). This situation is similar in the south Lapeiquan area, where the rocks exposed on opposite sides of the basin are different (Qinghai BGMR, 1986b). Thus, we suggest that the North Xorkol Basin conceals the trace of the paleo-ATF that was developed in the Oligocene. This reconstruction implies that the location of the main trace of the Altyn Tagh fault has changed since the Oligocene.

The unconformity between the folded Tertiary sediments below and the Lower Pleistocene conglomerates above provides evidence for basin inversion of the North Xorkol Basin in the Late Tertiary. Fission track dating (Wan et al., 2001; Chen, 2002; Chen et al., 2002b) also suggests a significant cooling, possibly related to tectonic activity that occurred at ~8 Ma in the Altyn Tagh region. This change is coeval with the end of basin filling in the North Xorkol Basin.

Initiation age of the Altyn Tagh fault

The initiation age of the ATF remains controversial (SSB, 1992; Rumelhart et al., 1997; Ge et al., 1998; Cui et al., 2001; Liu et al., 2001; Meng et al., 2001; Yue et al., 1999, 2001; Cowgill et al., 2000, 2003; Chen et al., 2001, 2002b, 2002c; Chen, 2002; Li et al., 2002b; Yin et al., 2002). Ge et al. (1998) proposed that the fault was initiated in the Late Paleocene. Li et al. (2002b) suggested that the major strike-slip movement along the Altyn Tagh fault zone started as early as Triassic time. $^{40}Ar/^{39}Ar$ laser dating of syntectonic muscovite and biotite from Jurassic rocks along the Altyn Tagh fault yields ages varying from 92 to 89 Ma (Liu et al., 2000). Yue and Liou (1999) and Yue et al. (2001) suggested a two-stage evolution model of the ATF in which the northeastern Altyn Tagh fault started to develop around Oligocene time. Yin et al. (2002) showed that at or prior to the Middle Eocene, the Altyn Tagh fault as a bounding structure of the Qaidam Basin was already in existence. Cowgill et al. (2000) suggested that both the Altyn Tagh fault and the North Altyn Tagh fault began strike slipping at the same time during the Oligocene and Miocene (2000). $^{40}Ar/^{39}Ar$ K-feldspar thermochronology for the central Altyn Tagh fault system by Cowgill et al. (2001) indicates that the ATF was already active as a left-lateral strike-slip fault in the Oligocene.

The oldest lithostratigraphy in those strike-slip basins along the central Altyn Tagh fault is Oligocene in age. Older strata may also exist, because we do not see the base of the stratigraphic section in the North Xorkol Basin. If the oldest lithostratigraphy in the strike-slip basin can represent the onset of those related to strike-slip faulting, then the Altyn Tagh fault must have started at or prior to the beginning of the Oligocene. Significant motion along the Altyn Tagh fault system is also supported by fission track ages of apatite from granites and gneiss across the Altyn Tagh range with ages varying from 35.6 Ma to 8 Ma (Chen et al., 2001, 2002b; Chen, 2002). Rapid changes of $\delta^{18}O$ and $\delta^{13}C$ values in calcite from the Jianggalesayi area, on the northwestern edge of the Altyn Tagh range (Fig. 1), starting in the Early Oligocene, also indicate that a significant uplift of mountain ranges took place during the Early Oligocene in the south (i.e., the Tibetan Plateau), creating a rain shadow (Chen, 2002; Chen et al., 2002c).

Magnitude of slip and slip rate along the Altyn Tagh fault

Correlation of the Yitunbulake Basin with the Kumutashi Basin and the outlet-offset of the Xorkol Basin provide constraints of 80–100 km fault displacement along the ATF. Based on our reconstruction, this 80–100 km offset began to be accumulated at 8 Ma. This age is earlier than the rapid deposition of sediments in the Qaidam Basin starting at ~5 Ma (Metivier et al., 1998). Our interpretation implies an average slip rate of 10–12.5 mm/yr for the ATF since 8 Ma. However, this estimate is quite uncertain, because tight constraints on the age of the sedimentation and the associated basin that is offset by the Altyn Tagh fault are lacking.

Our result of 80–100 km offset is significantly less than the 350–400 km offset estimated by Xu et al. (1999) and Zhang et al. (2001), based on correlation of Paleozoic tectonic units across the fault, and the 360 km offset estimated by Ritts and Biffi (2000) based on the restoration of Jurassic lake shorelines. Our result is broadly compatible with the earlier estimate of slip by Peltzer and Saucier (1996) who suggested 156 ± 40 km left-lateral offset along the Altyn Tagh fault since 10 Ma. Yue et al. (2003) recently also proposed 165 km of post-Early Miocene slip on the ATF.

Detailed field mapping by Yin et al. (1999) revealed a couple of dislocated Cenozoic back thrusts on both sides of the ATF, suggesting that the eastern part of the Altyn Tagh fault has accumulated 280 ± 30 km strike-slip since Early Oligocene time

(40–32 Ma), which yield an average slip rate of 7–9 mm/yr (Fig. 1). If the reconstruction is correct, the fault should have experienced 180–200 km displacement between the Oligocene and Middle Miocene (40–8 Ma), yielding an average slip rate of 5–6.5 mm/yr. Subsequently the fault has accumulated 80–100 km displacement between 8 Ma and the present, requiring an average slip rate of 10–12.5mm/yr. These inferences indicate that the slip rate of the Altyn Tagh fault may have increased with time.

Conclusions

Field observation and geological mapping show that the Cenozoic sedimentary sequence along the central ATF can be divided into three units depending on lithostratigraphy and unconformities, suggesting that the ATF experienced a four-stage strike-slip motion during the Cenozoic. Evidence from both sedimentation in Cenozoic basins and uplift of mountains suggest that the ATF began its sinistral strike-slip in the Early Oligocene. The offset of a Cenozoic original uniform strike-slip basin and the dislocation of the outlet of the Xorkol Basin indicated 80–100 km sinistral offset along the fault since 8 Ma; the average Late Cenozoic slip rate is 10–12.5 mm/yr.

Acknowledgments

This study was supported by the Major State Basic Research Program of People's Republic of China (No. 2001CB409808 and 2001CB7110013), the National Natural Science Foundation for Young Geologists (No. 40102022), and the U.S. National Science Foundation.

REFERENCES

Burchfiel, B. C., Deng, Q., Molnar, P., Royden, L. H., Wang, Y., Zhang, P., and Zhang W., 1989, Intracrustal detachment with zones of continental deformation: Geology, v. 17, p. 748–752.

Chen, X. H., Yin, A., George, G. E., Cowgill, E. S., Grove, M., Harrison, T. M., and Wang, X. F., 2003, Two phases of Mesozoic north-south extension in the eastern Altyn Tagh Range, northern Tibetan Plateau: Tectonics, v, 22(5), p. 1053 [10.1029/2001TC001336].

Chen, Z. L., 2002, Cenozoic strike-slip history of the central Altyn Tagh fault—new evidences from the sedimentary process and uplift of mountains; Ph.D. thesis, Chinese Academy of Geological Sciences, 76 p. (in Chinese with English abstract).

Chen, Z. L., Gao, J., Zhang, Y. Q., Wang, X. F., and Chen, X. H., 2002a, Electron Spin Resonance Dating of the Late Cenozoic deformation along the central Altun Fault: Geological Review, v. 48 (suppl.), p. 140–145 (in Chinese with English abstract).

Chen, Z. L., Wang, J. L., Wang, X. F., Chen, X. H., and Pan, J. H., 2002b, Rapid strike-slip of the Altyn Tagh fault at 8 Ma and its geological implications: Acta Geologica Sinica, v. 23, no. 4, p. 295–300 (in Chinese with English abstract).

Chen, Z. L., Wang, X. F., Feng, X. H., Wang, C. Q., Chen, X. H., and Liu, J., 2002c, New evidence from stable isotope for the uplift of mountains in northern edge of the Qinghai-Tibetan plateau: Sciences in China (E), v. 32 (suppl.), p. 1–10 (in Chinese with English abstract).

Chen, Z. L., Zhang, Y. Q., Wang, X. F., and Chen, X. H., 2001, Fission track dating of apatite constrains on the Cenozoic uplift of the Altyn Tagh mountain: Acta Geologica Sinica, v. 22, no. 5, p. 413–418 (in Chinese with English abstract).

CNPC (China National Petroleum Corporation Coordinated Group of the Tertiary Research), 1992, Correlation between the Tertiary strata in oil-gas-bearing areas of China and the typical sequence in Europe and America: Chinese Sciences Bulletin, v. 36, no. 6, p. 491–496.

Cowgill, E., Yin, A., Harrison, T. M., Grove, M., and Wang, X. F., 2001, Oligocene initiation of the central Altyn Tagh fault system inferred from ^{40}AR/^{39}Ar K-feldspar thermochronology: EOS (Transactions of the American Geophysical Union), v. 82, no. 47, p. F-1018.

Cowgill, E., Yin, A., Harrison, T. M., and Wang X. F., 2003, Reconstruction of the Altyn Tagh fault based on U-Pb geochronology: Role of back thrusts, mantle sutures, and heterogeneous crustal strength in forming the Tibetan plateau: Journal of Geophysical Research, v. 108 no. 7, p. 2346 [10.1029/2002JB002080].

Cowgill, E., Yin, A., Wang, X. F., and Zhang, Q., 2000, Is the North Altyn fault part of a strike-slip duplex along the Altyn Tagh fault system?: Geology, v. 28, p. 255–258.

Cui, J. W., Li, L., Yang, J. S., Yue, Y. J., Li, P. W., Zhang, J. X., and Chen, W., 2001, The Altun fault: Its geometry, nature, and mode of growth: Acta Geologica Sinica, v. 73, no. 3, p. 133–143 (in Chinese with English abstract).

Ge, X. H., Zhang, M. S., and Liu, Y. J., 1998, Scientific problems and research trends in studying the Altun fault: Modern Geology, v. 12, no. 3, p. 295–301 (in Chinese with English abstract).

Gehrels, G. E., Yin, A., and Wang, X. F., 2003a, Detrital zircon geochronology of the northeastern Tibet: Geological Society of America Bulletin, v. 115, p. 881–896.

______, 2003b, Magmatic history of the Altyn Tagh, Nan Shan, and Qilian Shan region of western China: Journal of Geophysical Research, v. 108, no. 9, p. 2423 [10.1029/2002JB001876].

Guo, S. M., and Xiang, H. F., 1998, Study on spatial-temporal distribution of the left-lateral offsets since Oligocene–Miocene of the Altyn Tagh fault system: Seismology and Geology, v. 20, p. 9–17 (in Chinese with English abstract).

Guo, Z. J., and Zhang, Z. C., 1998, Types and evolution of the Altyn Tagh strike-slip basins: Geological Review, v. 44, p. 357–364 (in Chinese with English abstract).

Huang, H.C., Huang, Q.H., and Ma, Y.S., 1996, Geology and oil and gas prediction of the Qaidam Basin. Beijing: Geological Publishing House, 108 p. (in Chinese with English abstract).

Li, H. B., Yang, J. S., Shi, R. D., Wu, C. L., Tapponnier, P., Wang, Y. S., Zhang, J. X., and Meng, F. C., 2002a, Determination of the Altyn Tagh strike-slip fault basin and its relationship with mountains: Chinese Science Bulletin, v. 47, p. 572–577.

Li, H. B., Yang, J. S., Xu, Z. Q., Wu, C. L., Wang, Y. S., Shi, R. D., Liou, J. G., Tapponnier, P., and Irelan, R. T., 2002b, Geological and chronological evidence of Indo-Chinese strike-slip movement in the Altyn Tagh fault zone: Chinese Science Bulletin, v. 47, p. 27–32.

Liu, Y. J., Ye, H., Ge, X., Chen, W., Liu, J., Ren, S., and Pan, H., 2001, Lasr probe $^{40}Ar/^{39}Ar$ dating of mica on the deformed rocks from Altyn Tagh and its tectonic implications, western China: Chinese Science Bulletin, v. 46, p. 322–325.

Liu, Z. C., Wang, J., Wang, Y. J., Sun, S. Y., Chen, Y. A., Zhang, J. X., Jiang, W. Y., Fan, L. S., Li, J. Q., Yang, F., Qu, P., and Chen, H. L., 1997, On lower Tertiary chronostratigraphy and climatostratigraphy of Mangyai Depression in western Qaidam Basin: Journal of Stratigraphy, v. 20, no. 2, p. 104–113 (in Chinese with English abstract).

Meng, Q. R., Hu, J. M., and Yang, F. Z., 2001, Timing and magnitude of displacement on the Altyn Tagh fault: Constraints from stratigraphic correlation of adjoining Tarim and Qaidam basins, NW China: Terra Nova, v. 13, p. 86–91.

Metivier, F., Gaudermer, Y., Tapponnier, P., and Meyer, B., 1998, Northeastward growth of the Tibet Plateau deduced from balanced reconstruction of two sedimentary basins: The Qaidam and Hexi corridor: Tectonics, v. 17, p. 823–842.

Meyer, B., Tapponnier, P. , Bourjot, L., Metivier, F., Gaudemer, Y., Peltzer, G., Guo., S., and Chen, Z., 1998, Crustal thickening in Gansu-Qinghai, lithospheric mantle subduction, and oblique, strike-slip controlled growth of the Tibet Plateau: Geophysical Journal International, v. 135, p. 1–47.

Meyer, B., Tapponnier, P., Gaudemer, Y., Peltzer, G., Guo, S., and Chen, Z., 1996, Rate of left-lateral movement along the eastern segment of the Altyn Tagh Fault, east of 96E (China): Geophysical Journal International, v. 124, p. 29–44.

Molnar, P., Burchfiel, B. C., Zhao, Z., Lian, K., Wang, S., and Huang, M., 1987, Geomorphic evidence for active faulting in the Altyn Tagh and northern Tibet and qualitative estimates of its contribution to the convergence of India and Eurasia: Geology, v. 15, p. 249–253.

Molnar, P., and Tapponnier, P., 1975, Cenozoic tectonics of Asia: Effects of continental collision: Science, v. 189, p. 419–426.

Peltzer, G., and Saucier, F., 1996, Present-day kinematics of Asia derived from geologic fault rates: Journal of Geophysical Research, v. 101, p. 27,943–27,956.

Peltzer, G., Tapponnier, P., and Armijo, R., 1989, Magnitude of late Quaternary left-lateral displacements along the northern edge of Tibet: Science, v. 246, p. 1285–1289.

Qinghai BGMR (Qinghai Bureau of Geology and Mineral Resources), 1986a, Geological map of the Mangya Sheet: Beijing, China, Geological Publishing House, scale 1:200,000, 121 p. (in Chinese).

Qinghai BGMR (Qinghai Bureau of Geology and Mineral Resources), 1986b, Geological map of the Eboliang Sheet: Beijing, China, Geological Publishing House, scale 1:200,000, 327 p. (in Chinese).

Qinghai BGMR (Qinghai Bureau of Geology and Mineral Resources), 1991, Geologic history of the Qinghai region: Beijing, China, Geological Publishing House, 662 p. (in Chinese with English abstract).

Ritts, B. D., and Biffi, U., 2000, Magnitude of post-Middle Jurassic (Bajocian) displacement on the central Altyn Tagh fault system, northwest China: Geological Society of America Bulletin, v. 112, p. 61–74.

Ritts, B. D., Yue, Y. J., and Graham, S. A., 2003, Oligocene–Miocene tectonics and sedimentation along the Altyn Tagh fault, northern Tibetan plateau: Analysis of the Xorkol, Subei, and Aksay basins [abs.]: Abstracts of the 18th HKT workshop, Monte Verita, Switzerland, p. 103.

Rumelhart, P. E., Yin, A., Cowgill, E., Butler, R., Zhang, Q., and Wang, X. F., 1999, Cenozoic vertical-axis rotation of the Altyn Tagh fault system: Geology, v. 27, p. 819–822.

Rumelhart, P. E., An, Y., Rick, B., and Zhang, Q., 1997, Oligocene initiation of deformation of northern Tibet: Evidence from the Tarim basin, NW China [abs.]: Geological Society of America Abstracts with Programs, v. 29, p. A-143.

Shen, Z. K., Wang, M., Li, Y., Jackson, D. D., Yin, A., Dong, D., and Fang, P., 2001, GPS study of crustal deformation associated with the Altyn Tagh fault system: Journal of Geophysical Research, v. 106, p. 30,607–30,621.

SSB (State Seismological Bureau), 1992, The Altyn Tagh active fault: Beijing, China: Seismological Publishing House, 319 p. (in Chinese with English abstract).

Tapponnier, P., and Molnar, P., 1977, Active faulting and tectonics in China: Journal of Geophysical Research, v. 82, p. 2905–2930.

Wan, J. L, Wang, Y., and Li, Q., 2001, FT evidence of northern Altyn uplift in Late Cenozoic: Bulletin of Mineralogy, Petrology, and Geochemistry, v. 20, p. 222–224 (in Chinese with English abstract).

Wan, J., Wang, Y. J., Liu, Z. C., Li, J. Q., and Xi, P., 1999, Cenozoic environmental evolution of the Qaidam basin and its implications for the uplift of the Tibetan Plateau and the drying of ventral Asia: Paleogeography, Paleoclimatology, Palaeoecology, v. 152, p. 37–47.

Wang, E., 1997, Displacement and timing along the northern strand of the Altyn Tagh fault zone, Northern Tibet: Earth and Planetary Science Letters, v. 150, p. 55–64.

Washburn, Z., Arrowsmith, J. R., Forman, L. S., Cowgill, E., Wang, X., Zhang, Y. Q., and Chen, Z. L., 2001, Late Holocene earthquake history of the central Altyn Tagh fault, China: Geology, v. 29, p. 1051–1054.

Xinjiang BGMR (Xinjiang Bureau of Geology and Mineral Resources), 1981a, Geological map of the Bashikaogong Sheet: Beijing, China, Geological Publishing House, scale 1:200,000, 236 p. (in Chinese).

______, 1981b, Geological map of the Xorkol Sheet: Beijing, China, Geological Publishing House, scale 1:200,000, 237 p. (in Chinese).

______, 1993, Geologic history of the Xinjiang Uygur Autonomous Region: Beijing, China: Geological Publishing House, 681 p. (in Chinese with English abstract).

Xiang, H. F., Guo, S. M., Zhang, W. X., and Zhang, B. L., 2000, River offset and slip rate of the east segment of Altun Tagh fault zone, Gansu, China since the Quaternary: Seismology and Geology, v. 22, no. 2, p. 129–138 (in Chinese with English abstract).

Xu, Z. Q., Yang, J. S., Zhang, J. X., and Cui, J. W., 1999, A comparison between the tectonic units on the two sides of the Altun sinistral strike-slip fault and the mechanism of lithospheric shearing: Acta Geologica Acta, v. 73, p. 193–205 (in Chinese with English abstract).

Yang, J. S., Xu, Z. Q., Zhang, J. X., Chu, J. Y., Zhang, R. Y., and Liou, J. Q., 2001, Tectonic significance of early Paleozoic high-pressure rocks in Altun-Qaidam-Qilian Mountains, northwest China, *in* Hendrix, M. S., and Davis, G. A., Paleozoic and Mesozoic tectonic evolution of central and eastern Asia: From continental assembly to intracontinental deformation: Geological Society of America Memoir, v. 194, p. 151–170.

Yin, A., Gehrels, G., Chen X., and Wang, X. F., 1999, Evidence for 280 km of Cenozoic left slip motion along the eastern segment of the Altyn Tagh fault system, western China [abs.]: EOS (Transactions of the American Geophysical Union), v. 80, p. F1018.

Yin, A., and Harrison, T. M., 2000, Geologic evolution of the Himalayan-Tibetan orogen: Annual Review of Earth and Planetary Sciences, v. 28, p. 211–280.

Yin, A., and Nie, S., 1996, A Phanerozoic palinspastic reconstruction of China and its neighboring regions, *in* Yin, A., and Harrison, T. M., eds., The tectonics of Asia: New York, NY, Cambridge University Press, p. 442–485.

Yin, A., Rumelhart P. E., Bulter, R., Cowgill, E., Harrison, T. M., Foster, D. A., Ingersoll, R. V., Zhang, Q., Zhou, X. Q., Wang, X. F., Hanson, A., and Raza, A., 2002, Tectonic history of the Altyn Tagh fault system in northern Tibet inferred from Cenozoic sedimentation: Geological Society of America Bulletin, v. 114, p. 1257–1295.

Yue, Y. J., and Liou, J. G., 1999, Two-stage evolution model for the Altyn Tagh Fault, China: Geology, v. 27, p. 227–230.

Yue, Y. J., Ritts, B. D. and Graham, S. A., 2001, Initiation and long-term slip history of the Altyn Tagh fault: International Geology Review, v. 43, p. 1087–1093.

Yue, Y. J., Ritts, B. D., Graham, S. A, Wooden, J., Gehrels, G., and Zhang, Z. C., 2003, Slowing extrusion tectonics: Lowered estimate of post-Early Miocene long-term slip rate for the Altyn Tagh fault, China [abs.], *in* Abstracts of the 18th Himalaya-Karakoram-Tibet workshop, Ascona, Switzerland, p. 134.

Zhang, J. X., Zhang, Z. M., Xu, Z. Q., Yang, J. S., and Cui, J. W., 2001, Petrology and geochronology of eclogites from the western segment of the Altyn Tagh, northwestern China: Lithos, v. 56, p. 187–206.